NASA CONTRACTOR REPORT

NASA CR-1327

THE TE_{01} MODE REFLECTION COEFFICIENT OF A GROUND-PLANE MOUNTED PARALLEL-PLATE WAVEGUIDE ILLUMINATING A REFLECTING SHEET

by L. L. Tsai and R. C. Rudduck

Prepared by
OHIO STATE UNIVERSITY
Columbus, Ohio
for Langley Research Center

NATIONAL AERONAUTICS AND SPACE ADMINISTRATION • WASHINGTON, D. C. • MAY 1969

NASA CR-1327

THE TE_{01} MODE REFLECTION COEFFICIENT OF A GROUND-PLANE MOUNTED PARALLEL-PLATE WAVEGUIDE ILLUMINATING A REFLECTING SHEET

By L. L. Tsai and R. C. Rudduck

Issued by Originator as Technical Report No. 1691-30

Prepared under Grant No. NGR 36-008-005 by
OHIO STATE UNIVERSITY
Columbus, Ohio

for Langley Research Center

NATIONAL AERONAUTICS AND SPACE ADMINISTRATION

For sale by the Clearinghouse for Federal Scientific and Technical Information
Springfield, Virginia 22151 – CFSTI price $3.00

ABSTRACT

The TE_{01} mode reflection coefficient is analyzed for a symmetric parallel-plate waveguide terminated in a ground plane and radiating into a perfectly reflecting sheet oriented normal to the guide axis. The method of analysis and calculated results are similar to those of the TEM mode analysis presented in a previous publication. The transmission between two identical waveguides facing each other is also analyzed.

CONTENTS

I. INTRODUCTION

The reflection coefficient of a TEM mode symmetric parallel-plate waveguide illuminating a perfectly conducting sheet has been analyzed by wedge diffraction techniques.[1-4] In order to complete the picture, the orthogonal polarization, i.e., the TE_{01} mode, will be considered in this report. The geometry of the problem is as shown in Fig. 1 where the conducting sheet is oriented normal to the guide axis. Only the ground-plane mounted guide will be considered. The method of analysis to be employed is similar to that in Ref. 3.

The analysis of this reflecting sheet problem can give insight into the basic diffraction behavior of small aperture antennas which radiate into overdense plasmas. This analysis is applicable for spacecraft reentry situations in which the plasma medium can be adequately modeled by a simple reflecting sheet. A by-product of the analysis for this reflecting sheet problem is the solution to a different problem: the transmission between identical waveguides.

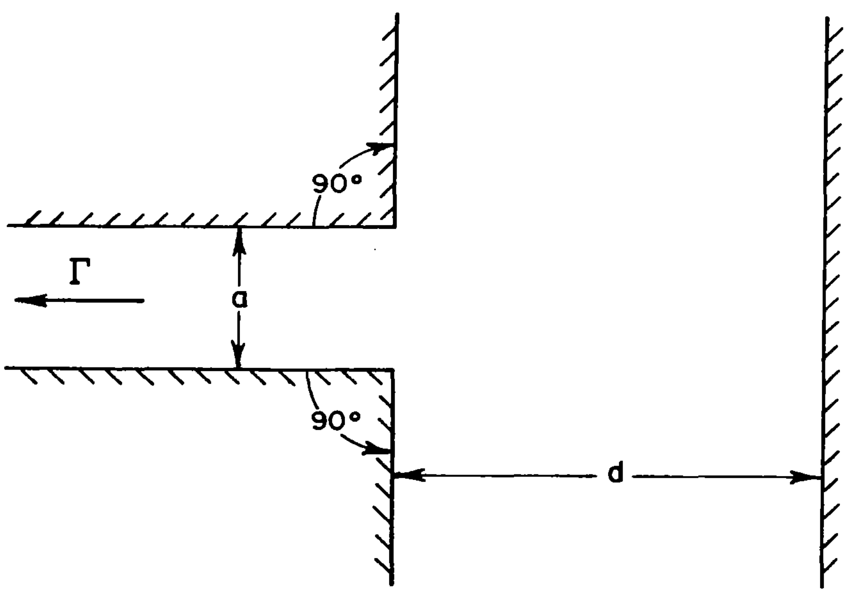

Fig. 1. Symmetric TE_{01} mode parallel-plate guide radiating into reflecting sheet.

II. REFLECTION COEFFICIENT ANALYSIS FOR THE GROUND-PLANE MOUNTED TE_{01} MODE GUIDE

By the wedge diffraction method the reflection coefficient of the waveguide is the superposition of the free space reflection coefficient (given in Ref. 5) and the reflection coefficient caused by the presence of the conducting sheet. The interaction between the guide and the reflector may be formulated in terms of successive bounce waves. The first bounce wave is the free space radiation from the waveguide which reflects from the sheet back onto the waveguide. This first bounce wave then scatters from the waveguide wedges producing a second bounce wave which propagates toward the reflecting sheet. The second bounce wave in turn reflects from the sheet back onto the waveguide giving rise to a third bounce wave, and so on to higher order bounces. Each bounce produces a contribution to the reflected TE_{01} mode in the waveguide.

Calculations of the free space fields of various parallel-plate guide configurations have been made[6] using both actual diffraction functions and limiting ray forms. These calculations show that in the region of the projected guide cross section the free space wave radiated from the guide may be represented by an isotropic cylindrical wave from an equivalent line source located at the center of the guide aperture. This and subsequent approximations in this analysis are valid provided the observation distances are sufficiently removed from the guide aperture. Typically, observation distances on the order of a few guide widths will yield very satisfactory results.

The equivalent cylindrical wave for the first bounce wave is given by the free space field on the axis of the guide; this field as analyzed by wedge diffraction may be obtained by summing the singly and doubly diffracted fields as discussed in detail in Ref. 6. The modal voltage of the equivalent line source representing the initial radiation from the guide may then be expressed as[7-8]

$$V_o = R_T(\theta=0)\,\frac{e^{-j\pi/2}}{\sqrt{k}} \qquad (1)$$

where $R_T(\theta=0)$ is the total on axis ray from the guide.[6]

Guide Scattering Properties

In order to analyze the multiple interactions between the guide and the reflecting sheet, the scattering properties of the guide must be examined first. For a plane wave of unit magnitude normally incident on the waveguide wedges as shown in Fig. 2 the diffracted field at a point P is given by

$$\text{(2)} \qquad E(P) = V_B(r_1, \psi_1 - \tfrac{\pi}{2}) - V_B(r_1, \psi_1 + \tfrac{\pi}{2}) + V_B(r_2, \psi_2 - \tfrac{\pi}{2}) - V_B(r_2, \psi_2 + \tfrac{\pi}{2}) + D_0^{(1)} \left[U_d(r_1, a, \psi_1, \pi) + U_d(r_2, a, \psi_2, \pi) \right],$$

where

$$\text{(3)} \qquad D_0^{(1)} = \frac{2}{3} \sin \frac{2\pi}{3} \left[\left(\cos \frac{2\pi}{3} - \cos \frac{\pi}{3}\right)^{-1} - \left(\cos \frac{2\pi}{3} - \cos \pi\right)^{-1} \right] \frac{e^{-j\frac{\pi}{4}}}{\sqrt{2\pi k}}$$

corresponds to the singly diffracted ray from each edge and

$$\text{(4)} \qquad U_d(r, r_0, \psi, \psi_0) = \frac{e^{-jk(r+r_0)}}{\sqrt{r+r_0}} \, e^{jk\left(\frac{r r_0}{r+r_0}\right)} \times \left[V_B\left(\frac{r r_0}{r+r_0}, \psi - \psi_0\right) - V_B\left(\frac{r r_0}{r+r_0}, \psi + \psi_0\right) \right]$$

is the diffracted field at (r, ψ) due to a line source at (r_0, ψ_0).[9] The V_B terms in Eq. (2) results from the singly diffracted waves from the wedges whereas the U_d terms express the doubly diffracted waves.

The formulation of the scattered field for the polarization of the TE_{01} mode (Eq. 2) differs from that of the TEM case (Eq. 9 in Ref. 3) only in the signs of the two V_B terms involving $\psi + \frac{\pi}{2}$. Consequently the same approximations used in Ref. 3 may be employed here.

Making the same approximations, i.e., small argument Fresnel Integral approximation and approximate shadow boundary diffraction functions, the same observation may be made for this polarization as was made in Ref. 3. Namely, the scattered field from the guide structure

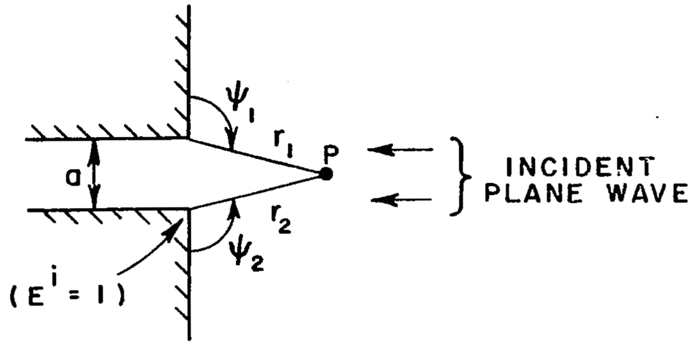

Fig. 2.. Scattering of an incident plane wave in the ground plane case.

due to plane wave incidence is composed of a reflected plane wave from the ground plane without the waveguide aperture present, denoted as the geometrical optics component; and an aperture component corresponding to the difference between the actual scattered field and the geometrical optics component. The aperture component is very similar to the backscatter by a strip or thick wall and may be represented in the projected guide cross section by an equivalent line source located at the center of the guide aperture.

For the case of cylindrical wave incidence as shown in Fig. 3 the aperture component of the scattered wave is, to a very good approximation, when the cylindrical source is sufficiently removed, the same as that for plane wave incidence as shown in Fig. 2, with the plane wave field equal to the incident field of the cylindrical wave at the waveguide aperture. The aperture component for cylindrical wave incidence is thus given by

(5) $$E_A = E^i K_A \frac{e^{-jkr_0}}{\sqrt{r_0}},$$

and

(6) $$K_A = \left[\frac{a}{\sqrt{\lambda}} e^{j\frac{\pi}{4}} - \frac{2}{9\pi} \sqrt{3\lambda}\, e^{-j\frac{\pi}{4}} + \frac{1}{1.5} \cot \frac{\pi}{1.5} \frac{e^{-j\frac{\pi}{4}}}{\sqrt{2\pi k}} \right] + 2 D_0^{(1)} \left[V_B(a, \tfrac{\pi}{2}) - V_B(a, \tfrac{3\pi}{2}) \right],$$

where E^i is the incident field of the cylindrical wave at the center of the aperture. The geometrical optics component for cylindrical wave incidence is simply the reflection of the incident cylindrical wave from the ground-plane without the guide aperture.

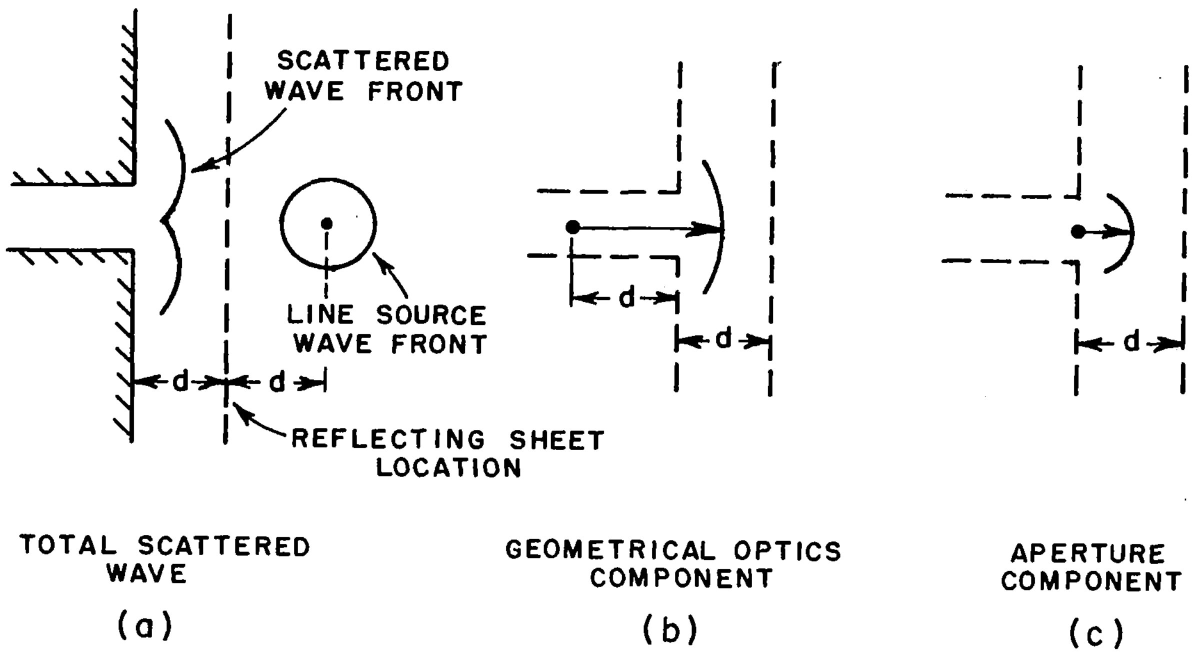

Fig. 3. Scattering of a cylindrical wave in the ground plane case.

Multiple Bounce Formulation

The formulation for the interactions or multiple bounces between the ground plane and reflecting sheet for the TE_{01} guide is analogous to that for the TEM guide in Ref. 3. Since the first bounce wave can be adequately described by an isotropic line source at the center of the aperture of the waveguide image, the first bounce contribution to the reflection coefficient is obtained as shown in Fig. 4a. Using the line source to waveguide coupling expression of Ref. 5, the contribution to the reflection coefficient of the guide from a line source located at a distance of r with modal voltage V^i is given by[8]

$$\Gamma = \frac{V}{V_0} = CV^i \frac{e^{-jkr}}{\sqrt{r}} , \tag{7}$$

where

$$C = \frac{\sqrt{\lambda}}{2a\cos A_0} \frac{R_T(\theta=0)\ e^{-j\pi/4}}{2\pi\sqrt{k}} , \tag{8}$$

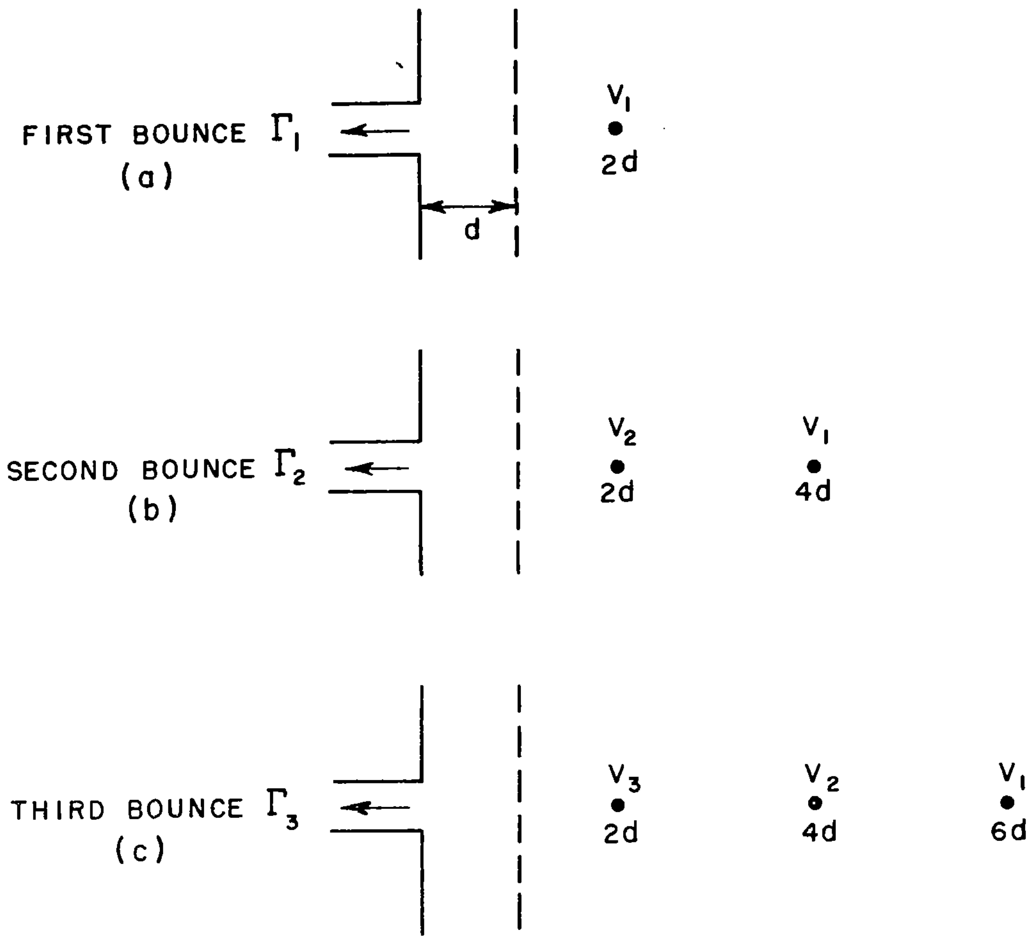

Fig. 4. Bounce contributions to reflection coefficient.

with $R_T(\theta=0)$ denoting the on axis ray of the guide. Thus the first bounce reflection coefficient contribution is given by

$$\Gamma_1 = CV_1 \frac{e^{-jk(2d)}}{\sqrt{2d}} \quad , \tag{9}$$

with the first bounce equivalent line source modal current given by

$$V_1 = - R_T(\theta=0) \frac{e^{-j\pi/2}}{\sqrt{k}} \quad , \tag{10}$$

where the minus sign results from the reflection by the reflecting sheet.

The scattering of the cylindrical wave from V_1 by the waveguide results in a second bounce wave which is composed of two components as shown in Fig. 3. The geometrical optics component of the second bounce wave reflects from the sheet back onto the waveguide such that it may be represented by the line source V_1 located at a distance 4d from the guide aperture, as shown in Fig. 4b. The aperture component of the second bounce wave reflects onto the waveguide as described by the line source V_2 in Fig. 4b. The value of V_2 is obtained by equating the value of its radiated field with that of the aperture component in Eq. (5)

(11) $$E_A = V_2 \frac{e^{-jkr_0 + j\frac{\pi}{4}}}{\sqrt{2\pi r_0}} = E^i K_A \frac{e^{-jkr_0}}{\sqrt{r_0}}$$

E^i is the incident field of the illuminating line source V_1 at the guide aperture in Fig. 4a, as given by

(12) $$E^i = V_1 \frac{e^{-jk(2d)+j\frac{\pi}{4}}}{\sqrt{2\pi(2d)}} \quad ,$$

Hence the value of V_2 is given by

(13) $$V_2 = - V_1 K_A \frac{e^{-jk(2d)}}{\sqrt{2d}} \quad ,$$

where the minus sign comes from reflection by the conducting sheet. The corresponding second bounce reflection coefficient is then given by the modal voltage induced by V_1 and V_2 as shown in Fig. 4b:

(14) $$\Gamma_2 = C \left[V_1 \frac{e^{-jk(4d)}}{\sqrt{4d}} + V_2 \frac{e^{-jk(2d)}}{\sqrt{2d}} \right] .$$

Generalizing, the n-th bounce wave is given by n cylindrical wave components with sources: V_1 at n(2d) , V_2 at (n-1) (2d), ----- V_n at (2d) The n-th source is given by

(15) $$V_n = - K_A \left[\sum_{m=1}^{n-1} V_m \frac{e^{-jk(n-m)2d}}{\sqrt{(n-m)2d}} \right] ,$$

and the n-th contribution to the reflection coefficient is given by

(16) $$\Gamma_n = C \left[\sum_{m=1}^{n} V_m \frac{e^{-jk2d(n-m+1)}}{\sqrt{2d(n-m+1)}} \right] .$$

The total reflection coefficient Γ of the waveguide is then obtained by superposing the guide's free space reflection coefficient[5] Γ_s and the reflection coefficient due to the reflecting sheet:

$$\Gamma = \Gamma_s + \sum_{n=1}^{\infty} \Gamma_n \quad . \tag{17}$$

<u>Results</u>

The total reflection coefficient for the TE_{01} mode ground-plane mounted guide was computed with the aid of the Fortran IV computer program presented in Appendix I. Figure 5 shows the calculated reflection coefficient magnitude for the case of guide width equal to 0.761λ while

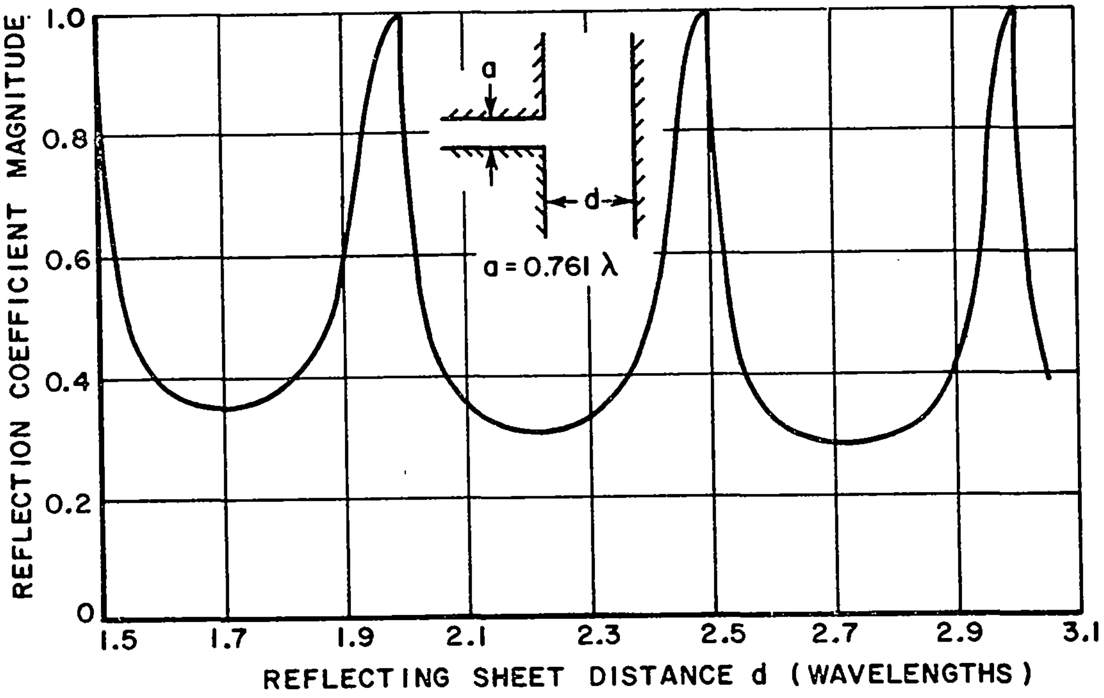

Fig. 5. Reflection coefficient magnitude for a ground-plane mounted TE_{01} mode parallel-plate waveguide illuminating a reflecting sheet.

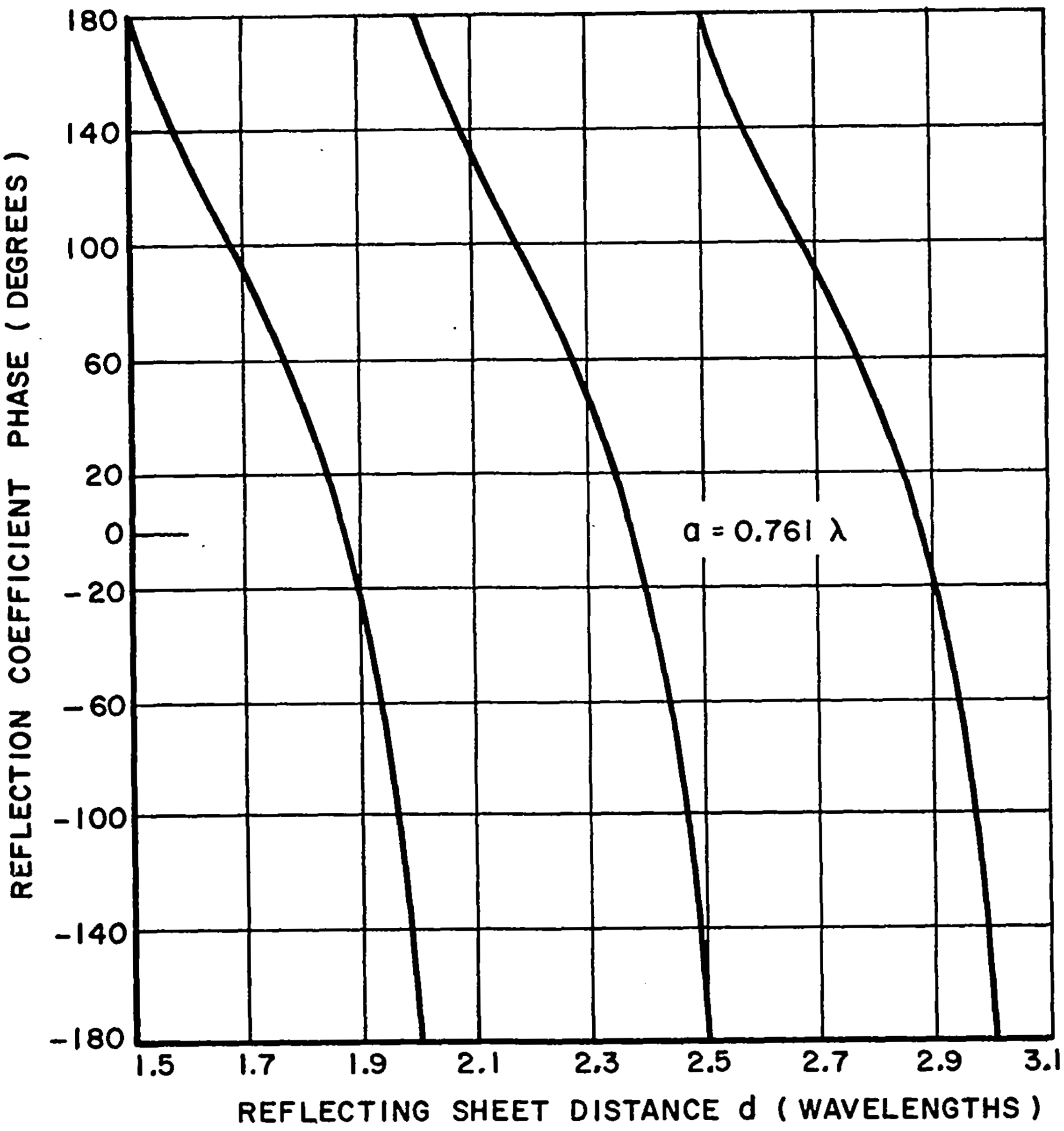

Fig. 6. Reflection coefficient phase.

Fig. 6 gives the corresponding phase for reflector spacings from 1.5λ to 3.0λ. The results for large reflector spacings, i.e., around 20.0λ, are shown in Fig. 7. The behavior of the reflection coefficient for the TE_{01} mode is essentially the same as that observed for the TEM mode[3]. At reflector spacings equal to integral mutiples of half wavelengths complete reflection is also observed for the TE_{01} mode excitation. This two-dimensional resonator phenomenon is confirmed by the existence of singularities at these cavity spacings in the Green's function for an electric line source located in a parallel-plate region as presented in Appendix II. As can be seen from Figs. 5 through 7 these cavity resonances become more localized as reflector spacing increases.

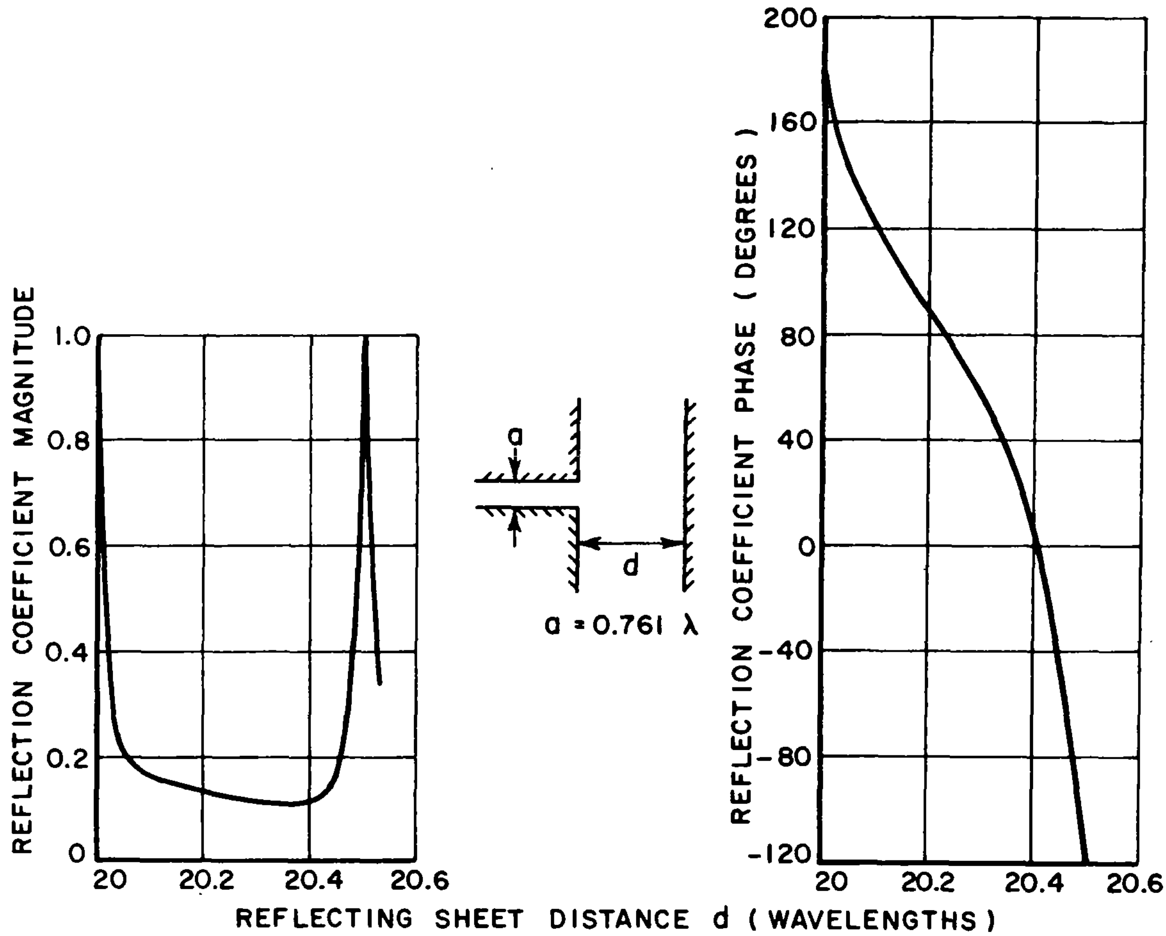

Fig. 7. Reflection coefficient for large reflector spacings.

The Transmission Problem

A by-product of the reflecting sheet problem is the solution for the transmission problem between two identical ground-plane mounted TE_{01} guides. Using image theory the negative of the sum of the odd number bounces gives the wave transmitted into the receiving guide while the sum of Γ_s with the negative of the even number bounces gives the reflection coefficient of the transmitting guide. Figures 8 and 9 give the magnitude and phase for the calculated transmission and reflection along with the reflection coefficient for the reflecting sheet problem. It may be seen that transmission peaks occur at every quarter wavelength in d.

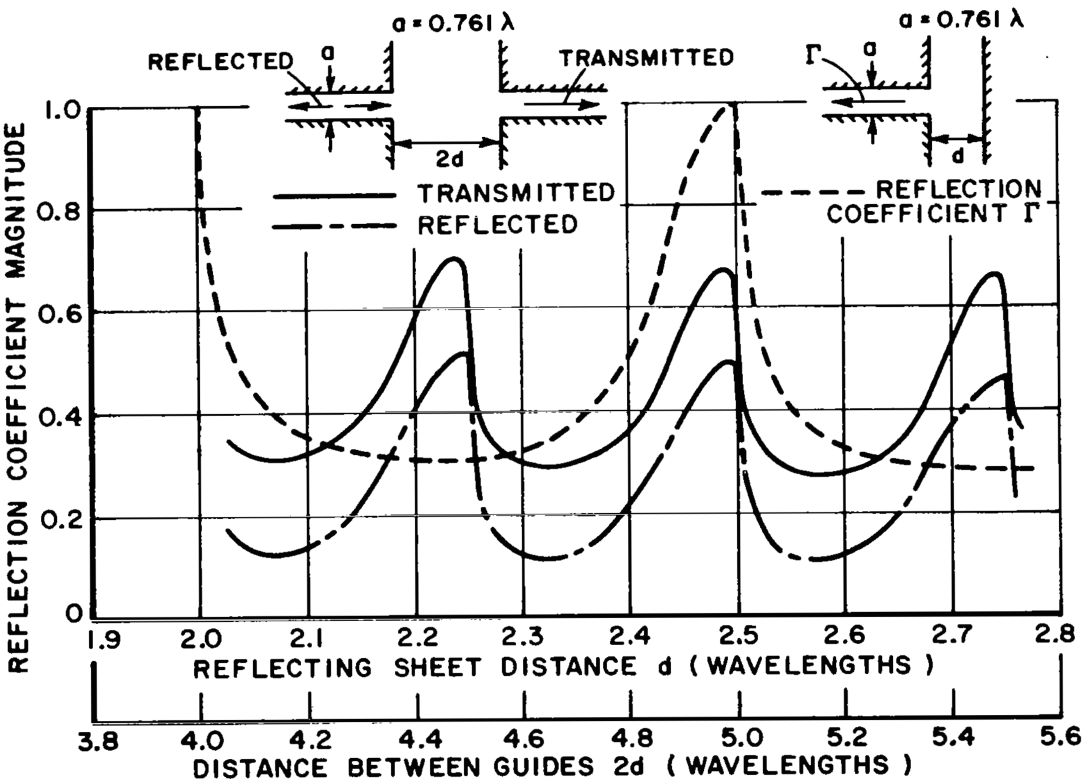

Fig. 8. The transmission problem presented with the reflecting sheet problem for a ground-plane mounted TE_{01} mode guide.

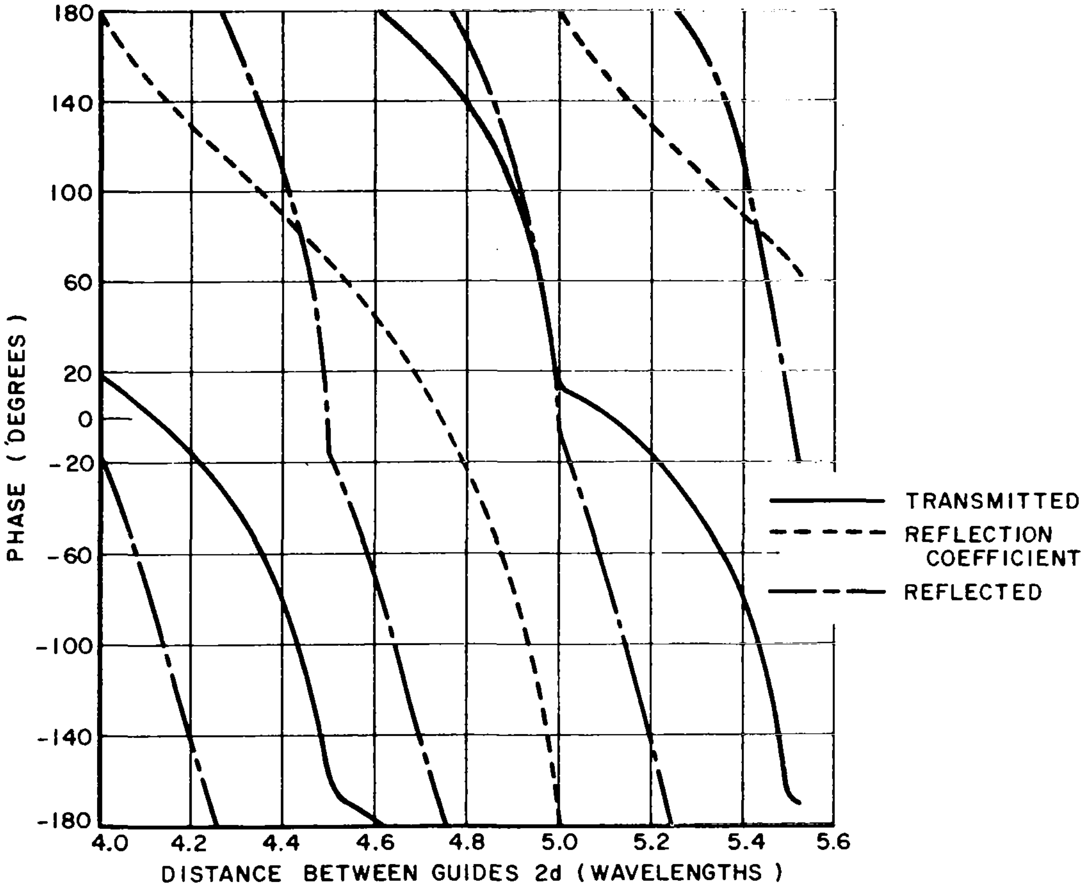

Fig. 9. The transmission and reflecting sheet problem phase.

III. CONCLUSIONS

The reflection coefficient of a TE_{01} mode symmetric parallel-plate waveguide mounted in a ground-plane and illuminating a perfectly reflecting sheet has been analyzed by wedge diffraction techniques. The interactions between the waveguide and reflector were described in terms of successively bouncing cylindrical waves. Summation of the contributions of the multiple bounces with the guide's free space reflection coefficient then yielded the total reflection coefficient.

Calculated reflection coefficients for this mode behave in essentially the same manner as those for the TEM mode in Ref. 3. At reflector spacings equal to integral multiples of $\lambda / 2$, resonance or complete reflection was observed. A by-product of this reflecting sheet problem was the solution of transmission between two identical TE_{01} guides facing each other.

APPENDIX I

A Fortran IV program used in the computation of the reflection coefficient is as follows:

```
C     TE01 GROUND PLANE GUIDE REFLECTION COEFFICIENT
      COMPLEX PFT,RD1,RDD1,RD1G,RT,GAMS,C,CTEMP,PPIF,XPIF,X,ABC,CBB,PGAM
     2,GAM,TEM,TEMP
      DIMENSION CUR(500),CUI(500),GAMR(500),GAMI(500)
      PI=3.1415927
      TWP=2.0*PI
      PFT=CEXP(CMPLX(0.0,-PI/4.0))/TWP
      READ (5,9) A,GAMS,NC
 9    FORMAT (3F10.6,I2)
      WRITE (6,11) A,GAMS
 11   FORMAT (20X,2HA=,F10.4,10X,5HGAMS=,2F10.6////)
      AOR=ARSIN(0.5/A)
      AO=180.0*AOR/PI
      STWP=SQRT(TWP)
      COPN=COS(PI/1.5)
      SIPN=SIN(PI/1.5)/1.5
      RTEMP=SIPN*(1.0/(COPN-COS((PI-AOR)/1.5))-1.0/(COPN-COS((PI+AOR)/1.
     25)))
      RD1=CMPLX(0.0,-RTEMP)
      RTEMP=SIPN*(1.0/(COPN-COS((0.5*PI-AOR)/1.5))-1.0/(COPN-COS((0.5*PI
     2+AOR)/1.5)))
      RD1G=CMPLX(0.0,-RTEMP)
      CALL VB (RVB1,UVB1,A,90.0,1.5)
      CALL VB (RVB2,UVB2,A,270.0,1.5)
      RDD1=RD1G*CMPLX(RVB1-RVB2,UVB1-UVB2)
      RT=2.0*(RD1+RDD1)
      WRITE (6,10) RD1,RD1G,RDD1,RT
 10   FORMAT (///1H ,5H RD1=,2E15.7,5X,5HRD1G=,2E15.7/1X,5HRDD1=,2E15.7,
     27X,3HRT=,2E15.7////)
      C=RT*PFT/SQRT(TWP)/(2.0*A*COS(AOR))
      CTEMP=-RT/SQRT(TWP)*CMPLX(0.0,-1.0)
      CUR(1)=REAL(CTEMP)
      CUI(1)=AIMAG(CTEMP)
      PPIF=CMPLX(0.70710678,0.70710678)
      XPIF=CONJG(PPIF)
      X=A*PPIF-2.0/(9.0*PI)*SQRT(3.0)*XPIF+1.0/1.5*COTAN(2.0943951)*XPIF
     2/TWP+2.0*RDD1*XPIF/TWP
      WRITE (6,50) C,X
 50   FORMAT (1H ,4E15.7)
      DO 200 I=1,NC
      READ (5,100) D,NB
 100  FORMAT(F10.5,I5)
      WRITE(6,74)A,D
 74   FORMAT (//1H ,12HGUIDE WIDTH=,F10.5,20X,18HREFLECTOR SPACING=,F10.
     25//)
      WRITE (6,77)
 77   FORMAT(1H ,15HGAMMA INCREMENT,15X,13HGAMMA BOUNCES,17X,11HGAMMA TO
     2TAL/)
C     ABC IS THE REFLECTED MODAL VOLTAGE
C     CBB IS THE TRANSMITTED MODAL VOLTAGE
      ABC=GAMS
      TD=2.0*D
      GAM=C*CMPLX(CUR(1),CUI(1))/SQRT(TD)*CEXP(CMPLX(0.,-TWP*TD))
      TEM=GAM
      PTEM=180./PI*ATAN2(AIMAG(TEM),REAL(TEM))
      GAMR(1)=REAL(GAM)+REAL(GAMS)
      GAMI(1)=AIMAG(GAM)+AIMAG(GAMS)
      CBB=-GAM
      AGAM=SQRT(GAMR(1)**2+GAMI(1)**2)
      PG=180./PI*ATAN2(GAMI(1),GAMR(1))
      N=1
      ATEM=CABS(TEM)
      WRITE (6,29) N,ATEM,PTEM,ATEM,PTEM,AGAM,PG
      DO 200 N=2,NB
```

```
      TEMP=CMPLX(0.,0.)
      NM=N-1
      XN=FLOAT(N)
      DO 156 M=1,NM
      XM=FLOAT(M)
      TEMP=-X*CMPLX(CUR(M),CUI(M))/SQRT(TD*(XN-XM))*CEXP(CMPLX(0.,-TWP*T
     2D*(XN-XM)))+TEMP
156   CONTINUE
      CUR(N)=REAL(TEMP)
      CUI(N)=AIMAG(TEMP)
      TEMP=CMPLX(0.,0.)
      XN=FLOAT(N)
      DO 157 M=1,N
      XM=FLOAT(M)
      TEMP=C*CMPLX(CUR(M),CUI(M))/SQRT(TD*(XN-XM+1.))*CEXP(CMPLX(0.,-TWP
     2*TD*(XN-XM+1.))))+TEMP
157   CONTINUE
      GAMR(N)=REAL(TEMP)
      GAMI(N)=AIMAG(TEMP)
      GAMR(N)=GAMR(N)+GAMR(N-1)
      GAMI(N)=GAMI(N)+GAMI(N-1)
      AGAM=SQRT(GAMR(N)**2+GAMI(N)**2)
      PGAM=CMPLX(GAMR(N),GAMI(N))-GAMS
      PTEM=180./PI*ATAN2(AIMAG(TEMP),REAL(TEMP))
      PG=180./PI*ATAN2(GAMI(N),GAMR(N))
      PPG=180./PI*ATAN2(AIMAG(PGAM),REAL(PGAM))
      ATEMP=CABS(TEMP)
      APGAM=CABS(PGAM)
      WRITE (6,29) N,ATEMP,PTEM,APGAM,PPG,AGAM,PG
29    FORMAT (5X,I5,5X,6E15.7)
      XXN=FLOAT (N)
      KHE=N/2
      XXY=XXN/2.0
      XKHE=FLOAT (KHE)
      IF (ABS(XXY-XKHE).GT.0.25) GO TO 573
      ABC=ABC-TEMP
      ABCM=CABS(ABC)
      ABCP=180.0/PI*ATAN2(AIMAG(ABC),REAL(ABC))
      GO TO 937
573   CBB=CBB-TEMP
      CBBM=CABS(CBB)
      CBBP=180.0/PI*ATAN2(AIMAG(CBB),REAL(CBB))
937   WRITE (6,29) N,ATEMP,PTEM,ABCM,ABCP,CBBM,CBBP
200   CONTINUE
201   CONTINUE
      STOP
      END
```

```
      SUBROUTINE VB (RVB,UVB,R,ANG,FN)
      COMPLEX DEM,TOP,COM,EXP,UPPI,UNPI
      DOUBLE PRECISION RAG,DP,TSIN
      PI=3.14159265
      TPI=6.28318530
      ANG=ANG*PI/180.0
      DEM=CMPLX(0.0,FN*SQRT(TPI))
      TOP=CEXP(CMPLX(0.0,-(TPI*R+PI/4.0)))
      COM=TOP/DEM
      N=IFIX((PI+ANG)/(2.0*FN*PI)+0.5)
      DN=FLOAT (N)
      A=1.0+COS(ANG-2.0*FN*PI*DN)
      BOTL=SQRT (TPI*R*A)
      EXP=CEXP(CMPLX(0.0,TPI*R*A))
      CALL FRNELS (C,S,BOTL)
      C=SQRT(PI/2.0)*(0.5-C)
      S= SQRT(PI/2.0)*(S-0.5)
      RAG=(PI+ANG)/(2.0*FN)
      TSIN=DSIN(RAG)
      TS=ABS(SNGL(TSIN))
      X=10.0
      Y=1.0/X**5
      IF(TS.GT.Y) GO TO 442
      COMP=-SQRT(2.0)*FN*SIN(ANG/2.0-FN*PI*DN)
      IF(COS(ANG/2.0-FN*PI*DN).LT.0.0) COMP=-COMP
      GO TO 443
442   DP=SQRT(A)*DCOS(RAG)/TSIN
      COMP=SNGL(DP)
443   UPPI=COM*EXP*COMP*CMPLX(C,S)
      N=IFIX((-PI+ANG)/(2.0*FN*PI)+0.5)
      DN=FLOAT(N)
      A=1.0+COS(ANG-2.0*FN*PI*DN)
      BOTL=SQRT(TPI*R*A)
      EXP=CEXP(CMPLX(0.0,TPI*R*A))
      CALL FRNELS (C,S,BOTL)
      C=SQRT(PI/2.0)*(0.5-C)
      S= SQRT(PI/2.0)*(S-0.5)
      RAG=(PI-ANG)/(2.0*FN)
      TSIN=DSIN(RAG)
      TS=ABS(SNGL(TSIN))
      IF(TS.GT.Y) GO TO 542
      COMP= SQRT(2.0)*FN*SIN(ANG/2.0-FN*PI*DN)
      IF(COS(ANG/2.0-FN*PI*DN).LT.0.0) COMP=-COMP
      GO TO 123
542   DP=SQRT(A)*DCOS(RAG)/TSIN
      COMP=SNGL(DP)
123   UNPI=COM*EXP*COMP*CMPLX(C,S)
      ANG=ANG*180.0/PI
      RVB=REAL (UPPI+UNPI)
      UVB=AIMAG(UPPI+UNPI)
      RETURN
      END
```

```
      SUBROUTINE FRNELS(C,S,XS)
      DIMENSION A(12),B(12),CC(12),D(12)
      A(1)=1.595769140
      A(2)=-0.000001702
      A(3)=-6.808568854
      A(4)=-0.000576361
      A(5)=6.920691902
      A(6)=-0.016898657
      A(7)=-3.050485660
      A(8)=-0.075752419
      A(9)=0.850663781
      A(10)=-0.025639041
      A(11)=-0.150230960
      A(12)=0.034404779
      B(1)=-0.000000033
      B(2)=4.255387524
      B(3)=-0.000092810
      B(4)=-7.780020400
      B(5)=-0.009520895
      B(6)=5.075161298
      B(7)=-0.138341947
      B(8)=-1.363729124
      B(9)=-0.403349276
      B(10)=0.702222016
      B(11)=-0.216195929
      B(12)=0.019547031
      CC(1)=0.0
      CC(2)=-0.024933975
      CC(3)=0.000003936
      CC(4)=0.005770956
      CC(5)=0.000689892
      CC(6)=-0.009497136
      CC(7)=0.011948809
      CC(8)=-0.006748873
      CC(9)=0.000246420
      CC(10)=0.002102967
      CC(11)=-0.001217930
      CC(12)=0.000233939
      D(1)=0.199471140
      D(2)=0.000000023
      D(3)=-0.009351341
      D(4)=0.000023006
      D(5)=0.004851466
      D(6)=0.001903218
      D(7)=-0.017122914
      D(8)=0.029064067
      D(9)=-0.027928955
      D(10)=0.016497308
      D(11)=-0.005598515
      D(12)=0.000838386
      IF(XS.LE.0.0) GO TO 414
      X=XS
      X=X*X
      FR=0.0
      FI=0.0
      K=13
      IF(X-4.0) 10,40,40
10    Y=X/4.0
20    K=K-1
      FR=(FR+A(K))*Y
      FI=(FI+B(K))*Y
      IF(K-2) 30,30,20
30    FR=FR+A(1)
      FI=FI+B(1)
```

```
      C=(FR*COS(X)+FI*SIN(X))*SQRT(Y)
      S=(FR*SIN(X)-FI*COS(X))*SQRT(Y)
      RETURN
40    Y=4.0/X
50    K=K-1
      FR=(FR+CC(K))*Y
      FI=(FI+D(K))*Y
      IF(K-2) 60,60,50
60    FR=FR+CC(1)
      FI=FI+D(1)
      C=0.5+(FR*COS(X)+FI*SIN(X))*SQRT(Y)
      S=0.5+(FR*SIN(X)-FI*COS(X))*SQRT(Y)
      RETURN
414   C=-0.0
      S=-0.0
      RETURN
      END
```

APPENDIX II

Morse and Feshback[10] give the Green's function for a magnetic line source in an infinite parallel-plate region derived from image theory. In this appendix, a Green's function will be derived following the method of Morse and Feshback for an electric line source in a parallel-plate region. Using the method of images as illustrated in Fig. 10, the Green's function for an electric line source located at (X_0, Y_0) is given by

$$G_k = \pi i \sum_{n=-\infty}^{\infty} \left[H_0 (k|\underline{r} - \underline{r}_n'|) - H_0 (k|\underline{r} - \underline{r}_n''|) \right] \tag{18}$$

$$= \pi i \sum_{n=\infty}^{\infty} \left\{ H_0\left[k \sqrt{(x - x_0 - 2nh)^2 + (y - y_0)^2} \right] - H_0\left[k \sqrt{(x + x_0 - 2nh)^2 + (y - y_0)^2} \right] \right\},$$

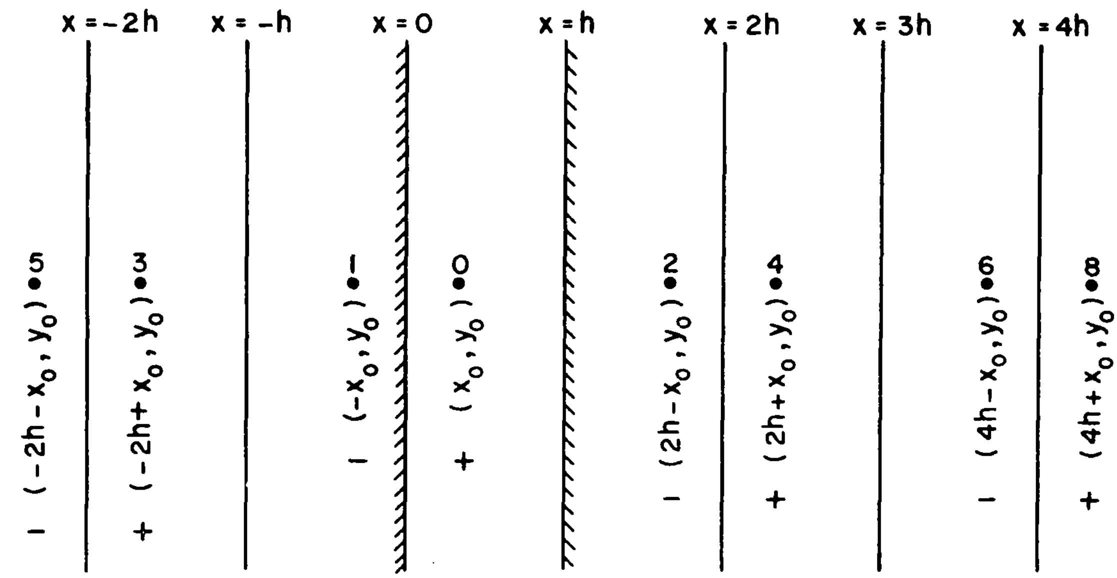

Fig. 10. Series of images for an electric line source in a parallel-plate region.

From Poisson's sum formula given by

$$(19) \qquad \sum_{-\infty}^{\infty} f(2\pi n) = \frac{1}{2\pi} \sum_{\nu=-\infty}^{\infty} F(\nu) \quad ,$$

where

$$(20) \qquad F(\nu) = \int_{-\infty}^{\infty} f(\tau)\, e^{-j\nu\tau}\, d\tau \quad ,$$

and the relationship[10]

$$(21) \qquad H_0 (k|\underline{r}-\underline{r}_0|) = \frac{i}{\pi^2} \int_{-\infty}^{\infty} dK_x \int_{-\infty}^{\infty} dK_y \left[\frac{e^{i\underline{K} \cdot (\underline{r}-r_0)}}{k^2 - K^2} \right] \quad ,$$

with $K^2 = K_x{}^2 + K_y{}^2$;
it then follows that we need to evaluate

$$(22) \qquad I = \int_{-\infty}^{\infty} e^{-j\nu\tau} \Big\{ H_0 \Big[k\sqrt{(x-x_0 - \tfrac{\tau}{\pi} h)^2 + (y-y_0)^2} \Big] - H_0 \Big[k\sqrt{(x+x_0 - \tfrac{\tau}{\pi} h)^2 + (y-y_0)^2} \Big] \Big\}\, d\tau.$$

Equations (18) and (22) differ from those in Ref. 10 only in sign, hence

$$(23) \qquad I = \left(\frac{4\pi}{ih}\right) e^{-i\pi\nu x/h} \sin\left(\frac{\pi\nu x_0}{h}\right) \frac{e^{i|y-y_0|\sqrt{k^2-(\pi\nu/h)^2}}}{\sqrt{k^2-(\pi\nu/h)^2}} \quad .$$

The final expression for the Green's function then becomes

$$(24) \qquad G_k(\underline{r}|\underline{r}_0) = \left(\frac{2\pi}{h}\right) \sum_{\nu=-\infty}^{\infty} e^{-i\pi\nu x/h} \sin\left(\frac{\pi\nu x_0}{h}\right) \cdot \frac{e^{i|y-y_0|\sqrt{k^2-(\pi\nu/h)^2}}}{\sqrt{k^2-(\pi\nu/h)^2}}$$

$$= \left(\frac{2\pi}{h}\right) \sum_{\nu=0}^{\infty} \epsilon_\nu \cos\left(\frac{\pi\nu x}{h}\right) \sin\left(\frac{\pi\nu x_0}{h}\right) \frac{e^{i|y-y_0|\sqrt{k^2-(\pi\nu/h)^2}}}{\sqrt{k^2-(\pi\nu/h)^2}}$$

From the above equation, we see that at $h=n\lambda/2$ where n = any integer, the Greens function for an electric line source in a parallel-plate region becomes singular and hence a resonance condition exists. This observation then serves to confirm the resonance behavior noted in Section II for an TE_{01} aperture opening into a parallel-plate cavity.

REFERENCES

1. Tsai, L. L., "The Reflection Coefficient of a TEM Mode Parallel-Plate Waveguide Illuminating a Perfectly Reflecting Sheet," Report 2143-1, 25 August 1966, ElectroScience Laboratory, The Ohio State University Research Foundation, prepared under Grant NGR-36-008-048, National Aeronautics and Space Administration, Office of Grants and Research Contracts, Washington, D. C.

2. Burnside, W.D., Tsai, L. L., and Rudduck, R. C., "The Reflection Coefficient of a TEM Mode Parallel-Plate Waveguide Illuminating a Conducting Sheet- the Large Wedge Angle Case," Report 2143-2, 2 February 1968, ElectroScience Laboratory, The Ohio State University Research Foundation; prepared under Grant NGR-36-008-048, National Aeronautics and Space Administration, Office of Grants and Research contracts, Washington, D. C. (NASA CR-1174, 1968).

3. Tsai, L. L., and Rudduck, R. C., "The Reflection Coefficient of a Ground-Plane Mounted TEM Mode Parallel-Plate Waveguide Illuminating a Conducting Sheet," Report 1691-27, 24 May 1968, ElectroScience Laboratory, The Ohio State University Research Foundation; prepared under Grant NGR 36-008-005, National Aeronautics and Space Administration, Office of Grants and Research Contracts, Washington, D. C.

4. Jones, J. E., Tsai, L. L., Rudduck, R. C., Swift, C. T., and Burnside, W.D., "The Admittance of a Parallel-Plate Waveguide Aperture Illuminating a Metal Sheet," to be published in the September 1968 issue of IEEE Transactions on Antennas and Propagation.

5. Rudduck, R. C., and Tsai, L. L., "Aperture Reflection Coefficient of TEM and TE_{01} Parallel-Plate Waveguides," IEEE Transactions on Antennas and Propagation, Vol. AP-16, No. 1., (January 1968), pp. 83-89.

6. Wu, D.C.F., Tsai, L.L., and Rudduck, R.C., "Equivalent Line Source Representations of Broadside Radiation from Parallel-Plate Waveguides", ElectroScience Laboratory report in processing.

7. Rudduck, R.C., "Application of Wedge Diffraction to Antenna Theory", Report 1691-13, 30 June 1965, Antenna Laboratory, The Ohio State University Research Foundation; prepared under Grant NsG-448, National Aeronautics and Space Administration Office of Grants and Research Contracts, Washington, D.C.

8. Tsai, L. L, and Rudduck, R. C., "The Influence of Conducting Flaps on the Reflection Coefficient of A Parallel-Plate Waveguide Illuminating a Conducting Sheet," Report 2143-5, 9 April 1968, ElectroScience Laboratory, The Ohio State University Research Foundation, prepared under Grant NGR-36-008-048, National Aeronautics and Space Administration, Office of Grants and Research Contracts, Washington, D. C.

9. Dybdal, R. B., Rudduck, R. C., and Tsai, L. L., "Mutual Coupling Between TEM and TE_{01} Parallel-Plate Waveguide Aperture," IEEE Transactions on Antennas and Propagation, Vol. AP-14, No. 5, (September 1966), pp. 574-580.

10. Morse, P. H., and Feshback, H., Methods of Theoretical Physics, McGraw-Hill, New York, N. Y., (1953), pp. 814-820.

NASA-Langley, 1969 —— 7